Small-signal analysis of spontaneous current instabilities in extrinsic semiconductors with trapping: Application to ultrapure *p*-type germanium

Luis L. Bonilla
*Dipartimento di Metodi e Modelli Matematici, Università di Padova, via Belzoni 7, 35131 Padova, Italy and Escuela Politécnica Superior, Universidad Carlos III de Madrid, Avenida del Mediterráneo s/n, 28913 Leganés, Madrid, Spain**

(Received 31 May 1991; revised manuscript received 16 December 1991)

An analysis of the spontaneous current instability in dc-voltage-biased extrinsic semiconductors is given. We use a standard rate-equation model of electrical conduction in long one-dimensional extrinsic semiconductors that includes effects of field-dependent impurity-impact ionization. The unique steady state is constructed and its current-voltage diagram characterized. It is shown that a negative differential resistance is necessary for linear instability of the steady state both above and below the field corresponding to impurity breakdown. We characterize the minimal sample length for oscillatory instability above the threshold field for impurity breakdown. The interval of voltages where the steady state is linearly unstable is then shown to belong to the relatively flat part of the steady current-voltage diagram. We comment on how our results may be related to recent observations on ultrapure *p*-type germanium.

I. INTRODUCTION

Semiconductors in which spontaneous bulk current instabilities occur have been shown to exhibit a wide range of temporal oscillatory and chaotic behavior under suitable bias conditions, including period-doubling and frequency-locking routes to chaos.[1–7] Quantitative verification of scaling predictions at the onset of chaos in voltage-biased *p*-type germanium at low temperature has been carried out with great accuracy.[5] Comparatively, the corresponding spatial structure of the current instabilities has received less attention until quite recently.[6–8]

Recent experimental work on the spatial structure of the current instabilities in dc-voltage-biased *p*-type Ge beyond the threshold for impurity breakdown has provided us with quite a detailed experimental characterization thereof.[6,7] Kahn, Mar, and Westervelt[6,7] have observed that a time-periodic current oscillation due to motion of domains sets in above a certain bias. This is similar to the classical Gunn oscillations in GaAs.[9–11] However, for *p*-type Ge there is an intermediate range between the voltages for which the current is constant and the higher voltage beyond which the current is purely time periodic. In this intermediate voltage range, the current switches intermittently between a small-amplitude oscillation at an approximate frequency of 6 Hz and large spikes caused by domain propagation.[7] At higher voltages, the spikes repeat themselves periodically causing an oscillation of the current at a frequency about four times lower.

In this paper we study a standard rate-equation model[12] near the threshold for oscillatory instability of a steady state, and use the results to interpret the experimental observations of Kahn, Mar, and Westervelt.[7] We find a reduced equation for the electric field valid both above and below breakdown, except in a narrow layer near the receiving contact where a different approximation holds; the shape of the unique steady state and of its current-voltage characteristic diagram; a minimal sample length criterion for current instability based upon a rough linear stability analysis of the steady state; the steady state is linearly unstable only in an interval of voltages corresponding to negative differential resistance (NDR); NDR is also necessary for linear instability of the steady state below breakdown, where different current instabilities are observed.[5,12] Given the absence of NDR below breakdown in the present model, the instabilities cannot rise as bifurcations from the steady state

Although we only give order of magnitude estimates and not precise quantitative results, it is hoped that our small-signal analysis will pave the way towards a more complete theoretical understanding of the behavior experimentally observed by Kahn, Mar, and Westervelt.[7]

Teitsworth[12] has used a rate-equation model to show that a region of NDR can occur in extrinsic photoconductors due to the combined effects of velocity saturation and field-dependent impact ionization. It is well known that dc-voltage-biased semiconductors with NDR in the plot of local current versus local electric field may be unstable to the formation of space-charge domains.[13] In a recent paper,[14] Bonilla and Teitsworth have constructed different traveling-wave solutions (periodic and solitary waves and monotonic wave fronts) of the model of Ref. 12 on the infinite one-dimensional line. Space-charge domains are either solitary waves or flat-top solutions bounded by monotonic wave fronts.[15,16] For the model of Ref. 12, the monotonic wave fronts are stable while the solitary waves are unstable under current bias.[17] Voltage-bias conditions cannot be enforced unless finite samples are considered, and therefore boundary conditions at the metallic contacts play a crucial role in the explanation of current instabilities.[10,11]

The model equations are[12,14]

$$\partial a_*/\partial T=\gamma a_0+p(\kappa a_0-r a_*),\quad a_0+a_*\equiv a=\text{const}\ , \tag{1.1a}$$

$$\epsilon\partial\tilde{E}/\partial T=J_{\text{tot}}(T)-e(pv_d-D\partial p/\partial X)\ , \tag{1.1b}$$

$$\epsilon\partial\tilde{E}/\partial X=e(p+d-a_*)\ . \tag{1.1c}$$

Here $\tilde{E}$ denotes the electric field, and $a_0\equiv a-a_*$, a_*, and p represent the neutral acceptor, ionized acceptor, and free hole concentrations, respectively. The total concentration of acceptor impurities is a const a. In (1.1a), γa_0 describes the generation of ionized from neutral acceptors by thermal and far-infrared radiation of appropriate wavelength; γ is proportional to the total photon flux. The rate of impact ionization of neutral acceptors is $p\kappa a_0$, and the rate of hole recombination onto ionized acceptors is pra_*. (1.1b) is Ampére's law, describing the balance between the hole current $e(pv_d-D\partial p/\partial X)$ and the displacement current $\epsilon\partial\tilde{E}/\partial T$. J_{tot} is the total current, equal to the current flowing through the external circuit because the displacement current in a metallic wire is negligible. Because of this identification, J_{tot} is sometimes called the external current. Finally, (1.1c) is Poisson's law for the electric field, in which the electric charge is given by the free hole, compensating donor (d), and ionized acceptor concentrations while ϵ is the semiconductor permittivity.[12] The hole diffusivity D is taken to be independent of the electric field and approximately determined by the Einstein relation $D=k_BT_0\mu_0/e$, where $\mu_0=dv_0/d\tilde{E}$ is the mobility at $\tilde{E}=0$, and T_0 is the lattice temperature. The drift velocity of the free holes, v_d and the recombination and impact ionization coefficients r and κ are all functions of the local electric field $\tilde{E}$, and are depicted in Fig. 1.[12,14]

Equations (1.1a)–(1.1c) have to be solved with appropriate boundary and initial conditions and with specified bias. dc voltage bias means

$$\int_0^L\tilde{E}(X,T)dX=-\tilde{V}\ . \tag{1.2}$$

As boundary conditions we adopt[18]

$$\tilde{J}_n(\tilde{E}(nL,T))=J_{\text{tot}}(T)-\epsilon\partial\tilde{E}/\partial T,\quad n=0.1\ , \tag{1.3a}$$

where $\tilde{J}_n(\tilde{E})$ is the contact conduction current density, having the same general properties as the control characteristic discussed by Kromer.[19] Equation (1.3a) specifies that no current is created or destroyed at the contacts: the contact conduction current density $\tilde{J}_n(\tilde{E})$ is equal to the hole current $e(pv_d-D\partial p/\partial X)$ which is the right-hand side of (1.3a) because of Ampère's law (1.1b). The main property of $\tilde{J}_n(\tilde{E})$ is its being an *increasing* function of $\tilde{E}$. This implies that the voltage drop at the injecting contact, $x=0$, increases with increasing $\tilde{J}_0$ for biases that make NDR possible (see below). The qualitative properties (shape and stability) of the steady states and domains[20] under dc voltage bias depend on where the curve $\tilde{J}_0(\tilde{E})$ intersects the bulk current-field characteristic curve we describe below. Thus a general increasing $\tilde{J}_0(\tilde{E})$ and an Ohmic-contact current density,

$$\tilde{J}_n(\tilde{E})=\tilde{E}/\tilde{\rho}_n,\quad \tilde{\rho}_n>0,\ n=0,1\ , \tag{1.3b}$$

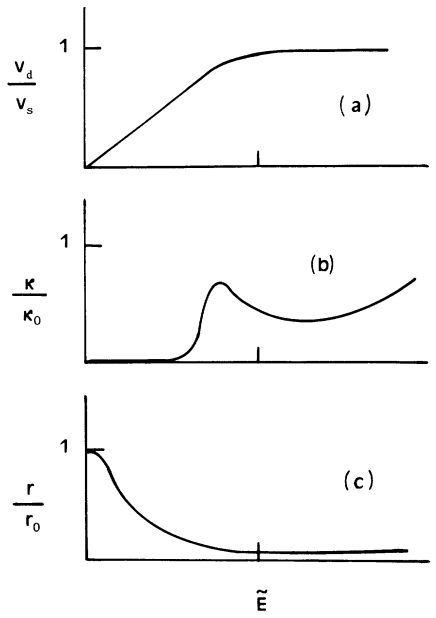

FIG. 1. Sketch of the electric-field dependence $\tilde{E}$ of (a) the hole drift velocity v_d; (b) the impurity-impact-ionization coefficient κ; and (c) the capture coefficient r. For p-type Ge, we have the following typical values $\tilde{E}=v_s/\mu_0\approx 10$ V/cm, $v_s\approx 10^7$ cm/s, $\kappa_0\approx 2.5\times 10^{-6}$ cm^3/s, and $r_0\approx 10^{-6}$ cm^3/s.

can be analyzed in the same way and these analyses will yield similar results. We adopt the simple Ohm's law (1.3b) in the rest of this paper, although we will comment upon the changes other boundary conditions would bring about in the pertinent places.

In Ref. 14 a theory of waves traveling on an infinite one-dimensional sample (with constant current bias) was obtained by using the large separation between the dielectric relaxation time and the characteristic time of ionization of the impurities: the impurity ionization is a much slower process than dielectric relaxation. The illumination rate does not count above the breakdown field, although it is a crucial process below threshold.[12] If we make Eqs. (1.1) dimensionless, so that time is measured in the slow scale of impurity ionization, they become[14] (see also Appendix A)

$$\partial A/\partial\tau=\Gamma(\alpha-1-A)/\beta+P[(\alpha-1)K-R-(K+R)A]\ , \tag{1.4a}$$

$$\beta\partial E/\partial\tau=J(\tau)-VP+\delta\partial P/\partial x\ , \tag{1.4b}$$

$$\partial E/\partial x=P-A\ . \tag{1.4c}$$

Here the coefficients V,K, and R are nondimensional analogs of v_d,r and κ, and therefore they are known as nonlinear functions of the electric field $E(x,\tau)$.[14] Equations (1.4) have to be solved with the boundary conditions

$$E(nl,\tau)=\rho_n[J(\tau)-\beta\partial E/\partial\tau],\quad n=0,1\ , \tag{1.5}$$

at the Ohmic contacts. ρ_n is the dimensionless resistivity of the contact at $x=nl$ ($n=0,1$). Under dc voltage bias,

$J(\tau)$ is determined by solving (1.4) and (1.5) together with the condition

$$\int_0^l E(x,\tau)dx = \phi \ . \tag{1.6}$$

Here ϕ is *minus* the dimensionless voltage (see Appendix A).

In Eqs. (1.4) we have the following relations among the parameters:[14]

$$\beta \ll \delta \ll 1, \quad \Gamma/\beta \ll 1 \ . \tag{1.7}$$

The rest of the paper is organized as follows. In Sec. II we analyze the uniform steady states of our model and then discuss the phenomena of impurity breakdown and of NDR. In Sec. III we derive reduced equations valid above and/or below breakdown except in a narrow boundary layer near the receiving contact. We find the unique nonuniform steady state under dc voltage bias in Sec. IV and describe its current-voltage characteristic diagram. Section V is devoted to a simplified linear stability analysis of the (nonuniform) steady state above and below breakdown, respectively. We discuss our results in Sec. VI. Appendix A contains our nondimensionalization of the equations and the definition of the parameters we use. Appendix B considers the linear stability of a nonuniform steady state.

II. STEADY STATES ON THE INFINITE LINE AND THE BREAKDOWN FIELD

Let us start analyzing the uniform steady states of Eqs. (1.2) for constant J. They are constant solutions of the system

$$P = A \ , \tag{2.1a}$$

$$J - PV = 0 \ , \tag{2.1b}$$

$$\Gamma(\alpha - 1 - A)/\beta + P[(\alpha-1)K - R - (K+R)A] = 0 \ . \tag{2.1c}$$

Multiplication of (2.1c) by V^2 and elimination of P and A by means of (2.1a) and (2.1b) yield the following expression for J:

$$\Gamma(\alpha-1)V^2/\beta + [(\alpha-1)K - R - \Gamma/\beta] \times VJ - (K+R)J^2 = 0 \ . \tag{2.2}$$

By solving (2.2), we find a function of the electric field

$$J = j(E) \ . \tag{2.3}$$

The function $j(E)$ becomes very steep near the so-called breakdown field E_{br} at which $dj/dE = \infty$. Instead of writing the (cumbersome) exact equations for E_{br}, we can use the smallness of the parameter Γ/β, together with (2.2), to obtain the approximate expression

$$(\alpha-1)K(E_{br}) - R(E_{br}) = 0 \ . \tag{2.4}$$

(2.4) is the Lambert criterion.[21] The local maximum of the function $K(E)$ gives rise to a NDR region of $j(E)$ above breakdown for a compensation ratio α close to 1 ($\alpha = a/d$ between 1 and 1.5, i.e., for a closely compensated semiconductor), as shown in Fig. 2. Numerical evaluation shows that the difference between the fields corresponding to the local maximum and minimum of $j(E)$ increases as α tends to 1.

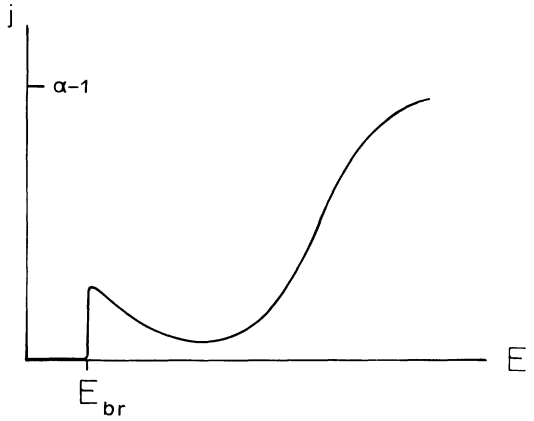

FIG. 2. Schematic graph of $j(E)$ vs electric field demonstrating NDR. $j(E)$ has a local maximum at (E_M, J_M) with $E_M \sim E_{br}$, a local minimum at (E_m, J_m) and it tends to $\alpha - 1$ for large values of E.

The main distinguishing feature of phenomena at each side of the breakdown is the order of magnitude of the current J. From Eq. (2.2) we see that, except in a small neighborhood of E_{br},

$$j(E) = \begin{cases} O(\Gamma/\beta) & \text{for } E < E_{br} \\ O(1) & \text{for } E > E_{br} \ . \end{cases} \tag{2.5}$$

Accordingly, it will be convenient to rescale the current when studying phenomena below breakdown. We thus expect that different equations approximate (1.4) at each side of E_{br}. They will be derived in Sec. III.

III. REDUCED EQUATIONS AT EACH SIDE OF BREAKDOWN

A. $E > E_{br}$

Let us assume that the voltage, boundary, and initial conditions conspire to keep $E > E_{br}$ throughout the semiconductor sample. Then we can obtain the leading-order approximation to Eq. (1.4) by equating all the small parameters β, δ, and Γ/β to zero. Thus we find

$$P = J(\tau)/V(E) \ ,$$

$$A = -\partial E/\partial x + J(\tau)/V(E) \ ,$$

which when inserted in Eq. (1.4a) yield the following hyperbolic equation [cf. Eq. (5.9) of Ref. 14]:

$$\partial^2 E/\partial x \partial \tau + c_1 \partial E/\partial \tau + c_2 \partial E/\partial x + c_3 = V^{-1} dJ/d\tau \ , \tag{3.1a}$$

$$c_1(E,J) = J(\tau)V'(E)/V(E)^2 \ , \tag{3.1b}$$

$$c_2(E,J) = J(\tau)[K(E) + R(E)]/V(E) \ , \tag{3.1c}$$

$$c_3(E,J)=(\{-1+\alpha K(E)/[K(E)+R(E)]\}V(E)-J(\tau))\times J(\tau)[K(E)+R(E)]/V(E)^2 . \quad (3.1d)$$

Equation (3.1) is to be solved with the boundary condition

$$E(0,\tau)=\rho_0 J(\tau) , \quad (3.2)$$

the bias condition

$$\int_0^l E(x,\tau)dx=\phi , \quad (3.3)$$

and given initial conditions. [The mathematical reason for keeping the boundary condition at the injecting contact and not at the receiving contact is that the wave solutions of (3.1a) on the whole real line propagate from left to right for $\phi>0$.[14] Thus what happens at $x=l$ depends on the input arriving from the bulk, whereas what happens at $x=0$ affects the field at the bulk.] Since the solution of the reduced problem (3.1)–(3.3) cannot, in general, satisfy the boundary condition at $x=l$, a diffusive boundary layer is attached there. In the boundary layer

$$(x-l)=O(\delta), \quad A\sim -1+\alpha K(E)/[K(E)+R(E)] ,$$

$$P\sim \partial E/\partial x ,$$

and therefore

$$\delta\partial^2 E/\partial x^2 \sim V(E)\partial E/\partial x, \quad \text{with } E(l,\tau)=\rho_1 J(\tau) , \quad (3.4a)$$

which yields

$$(x-l)/\delta \sim \int_{\rho_1 J(\tau)}^{E(x,\tau)} dE \left[\int_{E_{\text{out}}(l,\tau)}^{E} V(s)ds\right]^{-1} . \quad (3.4b)$$

$E_{\text{out}}(l,\tau)$ is the solution of the outer problem (3.1)–(3.3) evaluated at $x=l$. Notice that the boundary layer problem is quasistationary, so that time in (3.4b) enters as a parameter.

Remark 1. If ϕ is large enough so that $J\gg\Gamma/\beta$, Eq. (3.1) holds even if the resistivity is so small that $E<E_{\text{br}}$ at the contacts.

B. $E<E_{\text{br}}$

According to Eq. (2.5), E and $\partial E/\partial x$ are $O(1)$ and $J=O(\Gamma/\beta)$ if the voltage and the boundary conditions are such that $E<E_{\text{br}}$. From Eq. (1.4a) we then find $P=O(\Gamma/\beta)$. Thus $\beta\partial E/\partial\tau=O(\Gamma)$ can always be neglected whereas $\delta\partial P/\partial x=O(\delta\Gamma/\beta)$ can be ignored outside a boundary layer at $x=l$ (the receiving contact). The reduced equation valid for $0\le x<l$ is therefore obtained by setting δ and β (but not Γ/β) equal to zero in (1.4). The result is again Eq. (3.1a), where c_1 is still given by Eq. (3.1b), but now the coefficients c_2 and c_3 are

$$c_2(E,J)=\Gamma/\beta+J(\tau)[K(E)+R(E)]/V(E) , \quad (3.1e)$$

$$c_3(E,J)=\Gamma(\alpha-1)/\beta+J(\tau)[(\alpha-1)K(E)-R(E)]/V(E) . \quad (3.1f)$$

The reduced outer problem for fields below breakdown is therefore solving Eqs. (3.1a), (3.1b), (3.1e), and (3.1f), subject to the conditions (3.2) and (3.3) plus a given initial condition for the field. At $x=l$ the field is again obtained by means of (3.4b).

Remark 2. Notice that we can formally find a reduced outer problem that holds independent of the value of E (below or above breakdown). In fact, by setting the parameters δ and β equal to zero in Eqs. (1.4), we find Eqs. (3.1a) and (3.1b) together with

$$c_2(E,J)=\Gamma/\beta+J(\tau)[K(E)+R(E)]/V(E) , \quad (3.5a)$$

$$c_3(E,J)=\Gamma(\alpha-1)/\beta+J(\tau)[(\alpha-1)K(E)-R(E)-\Gamma/\beta]/V(E)-[J(\tau)/V(E)]^2[K(E)+R(E)] . \quad (3.5b)$$

Equations (3.5a) and (3.5b) become (3.1c) and (3.1d) above breakdown and (3.1a) and (3.1f) below breakdown, respectively.

Remark 3. Different scalings may be relevant if βl is not much smaller than 1 [$\beta l\ll 1$ for the experiments in p-type Ge (Refs. 5, 7, 12, and 14)]. For example, a slow scale $x=O(\beta)$ may be important if $\beta l\gg 1$ or even of order 1.

IV. STEADY STATES ON THE dc VOLTAGE BIASED FINITE SEMICONDUCTOR

We will find the stationary solutions to Eqs. (3.1a), (3.2), and (3.3) with the coefficients (3.1b), (3.5a), and (3.5b). These equations constitute an outer approximation to the original problem valid for all $E>0$, outside a narrow diffusive boundary layer at $x=l$. In the boundary layer the solution is approximately given by (3.4b).

The stationary solution satisfies

$$c_2(E,J)dE/dx=-c_3(E,J) , \quad (4.1a)$$

$$E(0)=\rho_0 J , \quad (4.1b)$$

$$\int_0^l E(x)dx=\phi . \quad (4.1c)$$

The steady state is therefore given by

$$x=-\int_{\rho_0 J}^{E(x)} J ds\, c_2(s,J)/c_3(s,J), \quad 0\le x<l , \quad (4.2)$$

with J determined by (4.1c). At $x=l$, $E=E(l)$ will, in general, be different from $\rho_1 J$, so that the boundary layer (3.4b) has to be inserted there. Note that these equations are identical to those of the steady states of the classical model of the Gunn effect in n-type GaAs.[11] We shall show below that the area under the steady state (4.2) (for each given J), $\Phi_{\text{ss}}(J)$, is an increasing function of J. Then

$$\Phi_{\text{ss}}(J)=\phi \quad (4.3)$$

has a unique solution $J_{\text{ss}}(\phi)$ which is itself an increasing function. This proves that *there is a unique dc voltage biased steady state for each* ϕ. Let us indicate now the qualitative shape of this state for different ϕ's and also what its current-voltage characteristic $J_{\text{ss}}(\phi)$ looks like.

Consider a long semiconductor with a compensation ratio such that $j(E)$ presents NDR above breakdown (Fig. 2). In the NDR region, Eq. (2.3) has three solutions

$E_i(J)$, $i=1,2,3$ with $E_1(J)<E_2(J)<E_3(J)$. (4.4)

Outside the NDR region, we will still call $E_1(J)$ $[E_3(J)]$ the solution of (2.3) on the first (respectively, third) branch of $j(E)$. Let us define now

$$\rho_{0M}=E_M/J_M \ , \tag{4.5a}$$

$$\rho_{0m}=E_m/J_m \ . \tag{4.5b}$$

Then we may distinguish three cases for the variation of the steady state with ϕ according to the value of the resistivity at $x=0$: A, $0<\rho_0<\rho_{0M}$; B, $\rho_{0M}<\rho_0<\rho_{0m}$; and C, $\rho_{0m}<\rho_0$.

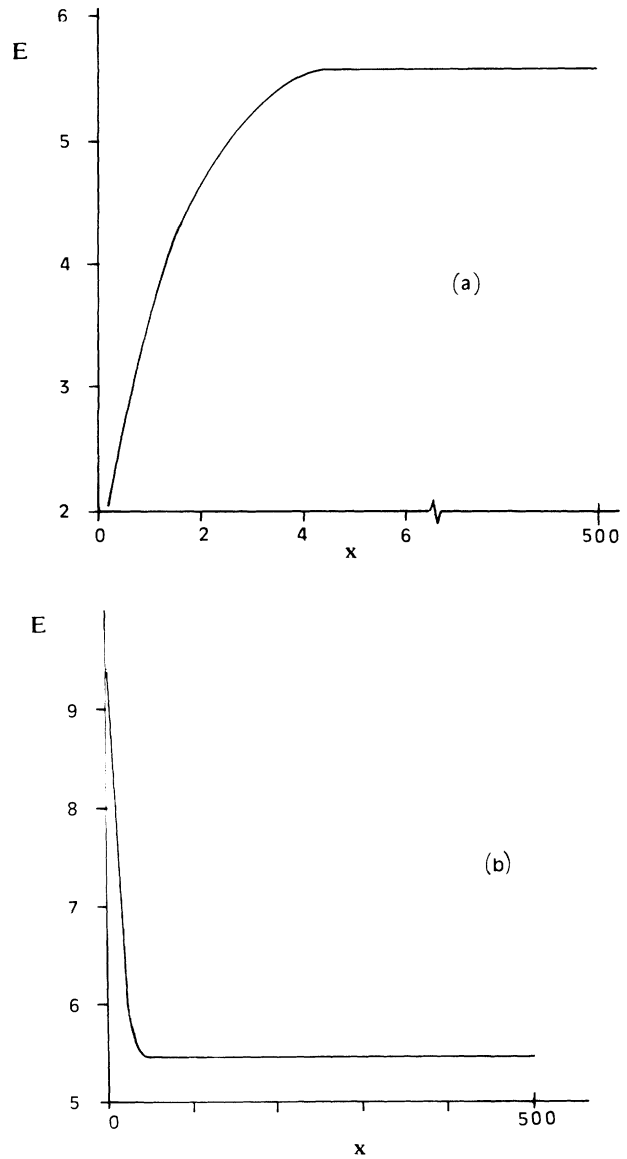

FIG. 3. Graphs of the electric field vs distance for the steady states. (a) $\rho_0 J<E_1$, or $E_2<\rho_0 J<E_j$; (b) $E_1<\rho_0 J<E_2$ or $\rho_0 J>E_3$. We have ignored the very narrow diffusive boundary layer at $x=l$. Numerical data correspond to $\alpha=1.4$, $l=500$, $\rho_0=3.817$, and for (a) $J=0.001$, while for (b) $J=0.25$. The scale for E has been multiplied by 10, which makes the unit equal to 1 V/cm, with our choice of nondimensional units. Notice the break in (a): E grows very fast until $E=E_1$ is reached.

A. Case A. $0<\rho_0<\rho_{0M}$

The curves $j(E)$ and E/ρ_0 either do not intersect, or they do so on the third branch of $j(E)$. If these curves do not intersect, the field at $x=0$ is always smaller than $E_1(J)$ or $E_3(J)$. Then $c_2>0$, $c_3<0$ in (4.1a) which implies $dE/dx>0$ for $x\geq 0$. The steady state is always as depicted in Fig. 3(a) for any $J>0$: it increases from $E(0)=\rho_0 J$ trying to reach $E_1(J)$ if $J<J_M$, or $E_3(J)$ if $J>J_M$. At $x=l$, $E(x)$ changes abruptly within the boundary layer from approximately $E_i(J)$ to its boundary value $\rho_1 J$. Clearly the area under the steady state, $\Phi_{ss}(J)$, grows with J as said above. The current-voltage characteristic $J_{ss}(\phi)$ is shown in Fig. 4, where the flat portion above breakdown corresponds to $J\sim J_M$. For consider the following.

(i) Below breakdown, $J=O(\Gamma/\beta)\ll 1$, which accounts for the almost zero value of $J_{ss}(\phi)$ in Fig. 4.

(ii) At breakdown, $E_1(J)\sim E_{br}$ for $J<J_M$, so that the area $\phi_{ss}(J)$ grows with J due to the increase of $E(0)=\rho_0 J$, and not to the increase of $E_i(J)$, the bulk value of $E(x)$. For a long semiconductor, $E(x)$ grows from $\rho_0 J$ to $E_1(J)$ in a layer of width $O(1)$ which is small compared to the length $l\gg 1$. Then in the breakdown region, the increase in the area $\phi_{ss}(J)$ due to the increase of J is modest, of order 1, when compared to the total area which is of the order of $E_{br}l$. Thus $\Phi_{ss}(J)$ varies little with J when $\phi\sim E_{br}l$, which means that the inverse function $J_{ss}(\phi)$ increases abruptly with ϕ when $\phi\sim E_{br}l$ as shown in Fig. 4.

(iii) The flat part of $J_{ss}(\phi)$ at $J=J_M$. For J slightly larger than J_M, the steady state has the following structure: a rapid increase [on a region of width $O(1)$] from

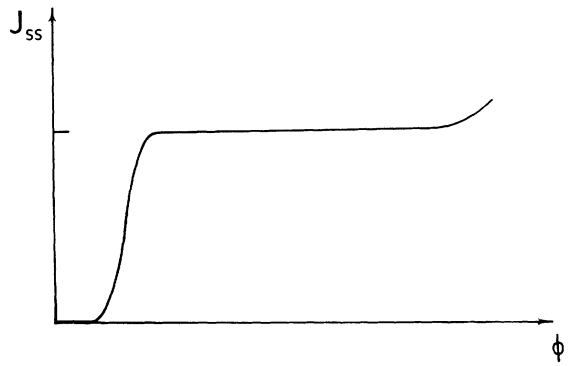

FIG. 4. Characteristic current-voltage diagram for the steady state. The flat portion is reached at a current $J=J_{crit}$ when $j=E/\rho_0$ and $j(E)$ intersect on the second (NDR) branch of the latter, $J=J_m$ when both curves intersect only on the first branch of $j(E)$; and $J=J_M$ when both curves do not intersect on the first two branches of $j(E)$. For $\alpha=1.4$, $l=500$, and $\rho_0=3.817$, the "flat" portion of $J_{ss}(\phi)$ has a slope which is twice and ten times smaller than that of the portions immediately following and preceding it, respectively.

$E(0)=\rho_0 J$ to $E_1(J_M)=E_M$, a flat portion of variable extension Δx; an $O(1)$ increase to $E\sim E_3(J_M)$ [assuming $E_1(J_M)$ and $E_3(J_M)$ to be of the same order]; and the $O(\delta)$ boundary layer at $x=l$. If $l\gg 1$, we may ignore the transition layers of $O(1)$ width and the narrower boundary layer. Then the steady state $E(x)$, of area $\phi\in(E_1(J_M)l, E_3(J_M)l)$ is $E=E_1(J_M)$, for $0<x<\Delta x$, and $E=E_3(J_M)$, for $\Delta x<x<l$, where

$$\Delta x=[E_3(J_M)l-\phi]/[E_3(J_M)-E_1(J_M)] . \quad (4.6a)$$

If $E_3(J_M)\gg E_1(J_M)$, the case of very closely compensated semiconductors $\alpha\downarrow 1$, the transition region between $E_1(J_M)$ and $E_3(J_m)$ cannot be ignored, and Δx is solution of the equation

$$E_1(J_M)\Delta x+\int_{\Delta x}^{l} E(x)dx=\phi . \quad (4.6b)$$

(iv) For $E_3(J_M)l<\phi$, $J_{ss}(\phi)$ increases again at a finite rate as shown in Fig. 4. When the lines E/ρ_0 and $j(E)$ intersect on the third branch of the latter, there is an interval of areas, (ϕ_1,ϕ_2), for which $\rho_0 J_{ss}(\phi)$ is larger than $E_3(J)$. Then $dE/dx<0$ and the steady state is as depicted in Fig. 3(b), still having an area $\Phi_{ss}(J)$ that increases with J.

(v) Note that in Fig. 4 we have exagerated the steepness of $J_{ss}(\phi)$ at breakdown (by ignoring variations of field in its neighborhood) and also its flatness at $J=J_M$ (by ignoring variations of current in its neighborhood). The transition layers of width $O(1)$ are more noticeable in smaller samples and tend to smooth out these effects.

B. Case B. $\rho_{0M}<\rho_0<\rho_{0m}$

E/ρ_0 and $j(E)$ intersect on the two first branches of the latter. Let J_b and J_{crit} be the currents at the corresponding intersection points.

$$E_1(J_b)=\rho_0 J_b , \quad (4.7)$$

$$E_2(J_{crit})=\rho_0 J_{crit} . \quad (4.8)$$

Arguments similar to those in case A show that $E(x)$ is as shown in Fig. 3(a) for $0<\phi<E_1(J_b)l, E_2(J_{crit})l<\phi<\phi_1, \phi>\phi_2$, and as shown in Fig. 3(b) for $E_1(J_b)l<\phi<E_2(J_{crit})l$ and $\phi_1<\phi<\phi_2$ [ϕ_1 and ϕ_2 correspond to the intersections of E/ρ_0 with the third branch of $j(E)$]. The current-voltage characteristic is as shown in Fig. 4 with the flat part of $J_{ss}(\phi)$ at $J=J_{crit}$ instead of J_M. An important difference is that the limits $J\uparrow J_{crit}$ and $J\downarrow J_{crit}$ have to be distinguished. When $E_1(J_{crit})l<\phi<E_2(J_{crit})l, J\uparrow J_{crit}$, and the steady state goes from a plateau $E=E_2(J_{crit})$ (for $0<x<\Delta x$) to another one with $E=E_1(J_{crit})$ (for $\Delta x<x<l$), through a transition region of width $O(1)$, where

$$\Delta x=[\phi-E_2(J_{crit})l]/[E_2(J_{crit})-E_1(J_{crit})] . \quad (4.9a)$$

When $E_2(J_{crit})l<\phi<E_3(J_{crit})l$, $J\downarrow J_{crit}$, and the steady state goes from a plateau $E=E_2(J_{crit})$ (for $0<x<\Delta x$) to another one with $E=E_3(J_{crit})$ (for $\Delta x<x<l$), through a transition region of width $O(1)$, where

$$\Delta x=[E_3(J_{crit})l-\phi]/[E_3(J_{crit})-E_2(J_{crit})] . \quad (4.9b)$$

If $E_3(J_{crit})\gg E_2(J_{crit})$ [or $E_2(J_{crit})\gg E_1(J_{crit})$], the case of very closely compensated semiconductors $\alpha\downarrow 1$, the transition region between $E_2(J_{crit})$ and $E_3(J_{crit})$ [or $E_2(J_{crit})$ and $E_1(J_{crit})$ for $J\uparrow J_{crit}$] cannot be ignored, and Δx is solution of the equation

$$E_2(J_{crit})\Delta x+\int_{\Delta x}^{l} E(x)dx=\phi$$
$$[\text{or } E_2(J_{crit})\Delta x+\int_{\Delta x}^{l} E(x)dx=\phi] . \quad (4.9c)$$

Note that when $E_1(J_b)l<\phi<E_2(J_{crit})l$ [Fig. 3(b)] there is a voltage drop near the injecting contact, as observed experimentally.[7]

C. Case C. $\rho_0>\rho_{0m}$

Then E/ρ_0 and $j(E)$ intersect only on the first branch of the latter, at a current given by (4.7). $E(x)$ is as depicted in Fig. 3(a) for $0<\phi<\rho_0 J_b l$, and as depicted in Fig. 3(b) for $\phi>\rho_0 J_b l$. The flat part in Fig. 4 is reached at $J\sim J_m$. Equation (4.6a) holds with J_m instead of J_M. If $E_3(J_M)\gg E_1(J_M)$, we have

$$\int_0^{\Delta x} E(x)dx+E_m(l-\Delta x)=\phi , \quad (4.10)$$

instead of (4.6b).

D. Other boundary conditions

A somewhat unphysical feature of our simple linear contact current density curve is the absence of a voltage drop for those voltages that give rise to a steady state with $dE/dx>0$ as shown in Fig. 3(a). It is very simple to remedy this situation if it is indeed experimentally checked that a voltage drop is present for all steady states below the threshold for instability. A possibility is to use

$$J_0(E)=\begin{cases}0, & \text{for } E<E_{br} ,\\ (E-E_{br})/\rho_0, & \text{for } E>E_{br} ,\end{cases} \quad (4.11)$$

with a resistivity such that $J_0(E)$ intersects $j(E)$ on its NDR branch. A motivation for this choice is the general formula used by Grubin[18] for the metal-semiconductor contacts used in Gunn effect experiments (see also p. 200 of Ref. 10):

$$\tilde{J}_0(\tilde{E})=-J_R\{\exp(-e\tilde{E}L_C/\nu k_B T_0)$$
$$-\exp[-(\nu^{-1}-1)e\tilde{E}L_C/\nu k_B T_0]\} . \quad (4.12)$$

Here ν is the ideality factor, that describes the contact as dominated by thermoionic emission ($\nu\approx 1$) or by tunneling ($\nu\gg 1$). J_R is the reverse flux that may be related to the barrier height through the Richardson equation. k_B is Boltzmann's constant and T_0 the lattice temperature. All the parameters in (4.12) except for L_C represent closely the properties of the metal-semiconductor interface. L_C gives an idea of the extension of the heavily doped contact region next to the metal-semiconductor interface[10] and it is a tunable parameter in Grubin's considerations.[18] By varying the three parameters ν, J_R, and L_C, it is possible to achieve a wide variety of shapes for $J_0(E)$, including sublinear and superlinear curves that go to infinity with E and also saturating curves that go to a cer-

tain finite limit as $E \to \infty$.[18] In particular, it is possible to achieve a sublinear $J_0(E)$ that intersects $j(E)$ only on its second (NDR) branch. This $J_0(E)$ would also give rise to steady states with a voltage drop [Fig. 3(b)] for $J < J_{\rm crit}$, just as the piecewise linear curve (4.11) above. The analysis of the steady state and its current-voltage characteristic is identical as that explained above and we omit it.

V. LINEAR STABILITY OF STEADY STATES

Here we analyze the stability of the steady states of the dc-voltage-biased Eq. (3.1). To simplify matters we shall ignore both the boundary layer region and the spatial structure of the steady state. While ignoring the boundary layer is justified because it contributes little to the integral of the field, we expect that ignoring the spatial structure of the steady field yields qualitatively valid results for long enough samples.[10] (Quantitatively valid results are obtained only for particular values of the voltage and of the contact resistivity at $x=0$.) Note that adopting piecewise linear versions of the coefficients in Eq. (3.1) does not lead to great simplifications, unlike what happens with the classical model for the Gunn effect in GaAs.[10] The reason is that the second-order partial derivative in (3.1a) (absent in the usual Gunn effect model) precludes using the flight time to analytically calculate the impedance.[10] Thus the calculations that follow are the simplest ones one can perform short of numerical solution of the model. (See also Appendix B.)

Let $E=E_s$ be the constant steady state corresponding to a (minus) voltage ϕ and $J_s=j(\phi/l)$ the corresponding current. Then let

$$E(x,\tau)=E_s+\varepsilon\hat{e}(x)\exp(\lambda\tau)\ , \tag{5.1a}$$

$$J(\tau)=J_s+\varepsilon\exp(\lambda\tau),\quad \varepsilon\ll 1\ . \tag{5.1b}$$

The linearized equation for $\hat{e}(x)$ is

$$(\lambda+c_2)d\hat{e}/dx+(\lambda c_1+c_4)\hat{e}=\lambda/V+c_5\ . \tag{5.2a}$$

Here c_1 and c_2 are as in Eqs. (3.1b) and (3.5a) evaluated at $E=E_s$ and $J=J_s$, while c_4 and c_5 are defined as the following functions also evaluated at $E=E_s$ and $J=J_s$:

$$c_4\equiv\partial c_3(E,J)/\partial E\ , \tag{5.2b}$$

$$c_5\equiv-\partial c_3(E,J)/\partial J\ . \tag{5.2c}$$

Note that all coefficients in (5.2a) are positive except for c_4 which may be negative above the breakdown field, thus providing the NDR.[14] c_4 has the same sign as dj/dE, the slope of the function $j(E)$. In fact, by use of the implicit-function theorem,

$$dj/dE=c_4/c_5\ (c_5>0),\quad \text{with } c_3(E,j(E))=0\ . \tag{5.3}$$

Equation (5.2a) is to be solved together with the boundary condition corresponding to (3.2) for $\hat{e}(x)$, namely,

$$\hat{e}(0)=\rho_0\ . \tag{5.2d}$$

The solution of Eq. (5.2) is

$$\hat{e}(x)=(\lambda/V+c_5)/(\lambda c_1+c_4)+[\rho_0-(\lambda/V+c_5)/(\lambda c_1+c_4)]\exp(-\Lambda x/l)\ , \tag{5.4a}$$

$$\Lambda=(\lambda c_1+c_4)l/(\lambda+c_2)\ . \tag{5.4b}$$

Insertion of (5.1a) and (5.4a) into the voltage bias condition (3.3) tells us that Λ has to be zero of the impedance $Z(\Lambda)$:

$$Z(\Lambda)=[(c_4-c_1c_5V)l+(c_5V-c_2)\Lambda][V(c_4-c_1c_2)]^{-1}\times l(\Lambda+e^{-\Lambda}-1)/\Lambda^2-\rho_0 l(e^{-\Lambda}-1)/\Lambda\ . \tag{5.5a}$$

λ is obtained from a zero of the impedance by inverting the relation (5.4b),

$$\lambda=(c_4l-c_2\Lambda)/(\Lambda-c_1l)\ . \tag{5.6}$$

For $E>E_{\rm br}$, c_5V is equal to c_2 up to terms of order Γ/β. Then we can simplify (5.5a) to

$$Z(\Lambda)=l^2V^{-1}[(\Lambda-e^{-\Lambda}-1)-a\Lambda(e^{-\Lambda}-1)]/\Lambda^2\ ,\qquad a\equiv\rho_0V/l\ . \tag{5.5b}$$

The zeros of $Z(\Lambda)$ are the nonvanishing zeros of $\Lambda^2Z(\Lambda)$. But this latter function is an exponential polynomial in $(-\Lambda)$ without a principal term.[22] Then it has an unbounded number of zeros with arbitrarily large $\mathrm{Re}\Lambda<0$ (Ref. 22, Theorem 13.1). The crucial thing is now whether $\Lambda^2Z(\Lambda)$ has zeros with positive real part. We now show that for both $E>E_{\rm br}$ and $E<E_{\rm br}$ all zeros of $Z(\Lambda)$ have negative real part, and then analyze the consequences of this fact.

A. $E>E_{\rm br}$

Let us start with the case of $E>E_{\rm br}$, Eq. (5.5b), and define $F(\Lambda)\equiv\Lambda^2Z(\Lambda)V/l^2$. It is important at this time to check that $\mathrm{Re}F(i\omega)$ and $\mathrm{Im}F(i\omega)$ are even and odd functions of $\omega\in\mathbb{R}$, respectively, and that

$$\mathrm{Im}F(i\omega)=\omega-\sin\omega+a\omega(1-\cos\omega)>0\quad\text{for }\omega>0 \tag{5.7a}$$

$$F(\Lambda)\sim(1+a)\Lambda\ \text{as}\ \Lambda\to\infty\quad\text{with Re}\Lambda>0\ . \tag{5.7b}$$

Then the principle of the argument[22] shows that $F(\Lambda)$ does not have any zeros with positive real part. Therefore $F(\Lambda)$ has infinitely many zeros with negative real part (which may be arbitrarily large). In the simple case of ideal Ohmic boundary conditions $a=0$, $F(\Lambda)$ coincides with the exponential polynomial studied by McCumber and Chynoweth in their analysis of the Gunn effect in GaAs.[23] Then all the zeros of $F(\Lambda)$ are simple and may be ordered starting with that with largest real part, namely

$$\Lambda_1\equiv\mu_1+i\omega_1\approx-2.09\pm i7.46\ . \tag{5.8}$$

By using the implicit-function theorem it can be shown that the real part of the zeros of $F(\Lambda)$ increases with a.

B. $E<E_{\rm br}$

Consider now $E<E_{\rm br}$ and define

$$F(\Lambda)\equiv(1+b\Lambda)(\Lambda+e^{-\Lambda}-1)-c\Lambda(e^{-\Lambda}-1)$$
$$=(\Lambda/l)^2Z(\Lambda)V(c_4-c_1c_2)/(c_4-c_1c_5V)\ , \qquad (5.9a)$$

$$b\equiv(c_5V-c_2)/[l(c_4-c_1c_5V)],\quad \mathrm{sgn}b=\mathrm{sgn}(dj/dE)\ , \qquad (5.9b)$$

$$c\equiv\rho_0V(c_4-c_1c_2)/[(c_4-c_1c_5V)l]>0\ . \qquad (5.9c)$$

Above impurity breakdown $b=0$, $c=a$, and (5.9a) coincides with (5.5b). From Eq. (5.9a) we derive the relations

$$\mathrm{Re}[F(i\omega)]=-(1-\cos\omega)-b\omega(\omega-\sin\omega)-c\omega\sin\omega\ , \qquad (5.10a)$$

$$\mathrm{Im}[F(i\omega)]=\omega-\sin\omega-(b-c)\omega(1-\cos\omega)\ , \qquad (5.10b)$$

$$F(\Lambda)\sim b\Lambda^2 \text{ as } \Lambda\to\infty \text{ with } \mathrm{Re}\Lambda>0\ . \qquad (5.10c)$$

For values of b and $c\geq 0$, we can use the principle of the argument[22] to show that the only non-negative zero of $F(\Lambda)$ is the irrelevant $\Lambda=0$. In fact, let us first consider $(b-c)<(1-2/\pi)$. We immediately see that

$$\mathrm{Im}[F(i\omega)]>0 \text{ for } \omega>0 \text{ if } (b-c)<1-2/\pi\ . \qquad (5.10d)$$

The image by $F(\Lambda)$ of the right half complex plane Λ excluding the origin, Fig. 5(a), does not enclose the origin of the complex plane $F(\Lambda)$ because $\mathrm{Im}F(i\omega)$ never vanishes, see Fig. 5(b). Then no zeros of $F(\Lambda)=Z(\Lambda)$ have positive real part. Let $(b-c)>(1-2/\pi)$. Then $\mathrm{Im}F(i\omega)$ may vanish. However, rewriting (5.10a) as

$$\mathrm{Re}[F(i\omega)]=-(1-\cos\omega)-b\omega[\omega-(1-c/b)\sin\omega]\ ,$$

it is clear that $\mathrm{Re}[F(i\omega)]$ is always negative $(0<b-c<b)$. Thus the image of the curve enclosing the right half plane (minus the origin) will not enclose the origin of the complex F plane [Fig. 5(c)]. Then the principle of the argument[22] implies that no zeros of $F(\Lambda)$ with positive real part exist.

C. Consequences

We now describe the consequences of our results. The first one is that a NDR is needed for linear instability of the steady state both above and below breakdown. Then the steady state is linearly stable below breakdown because $dj/dE>0$ (Fig. 2), and any instabilities observed there cannot arise as bifurcations from the steady state.

In fact, the steady state becomes oscillatory unstable at a field $E_s\sim\phi/l$ corresponding to $\mathrm{Re}\lambda=0$ in (5.6), with $\Lambda_1=\mu_1+i\omega_1$ being the zero of $Z(\Lambda)$ with largest real part [i.e., (5.8) for $\rho_0=0$]:

$$c_4(E_s,J_s)=c_2(E_s,J_s)\{\mu_1-\omega_1^2/[c_1(E_s,J_s)l-\mu_1]\}/l<0\ . \qquad (5.11)$$

Then a negative slope of the curve $j(E)$—that is, a region of NDR—is necessary for the steady state to become unstable $(dj/dE=c_4/c_5, c_5>0)$. Let σ be $|dj/dE|$ in the NDR region. Solving (5.11) for l and minimizing the result with respect to the electric field, we find the *minimal sample length* necessary to support a (linearly) unstable steady state

$$l>l_m\ . \qquad (5.12a)$$

Here l_m is the minimum of the positive solution of Eq. (5.12b) below for fields on the NDR region,

$$\sigma c_1c_5l^2+|\mu_1|(\sigma c_5-c_1c_2)l-c_2(\mu_1^2+\omega_1^2)=0\ . \qquad (5.12b)$$

Note that the solution of (5.12b) decreases when σ increases. Above breakdown, (5.12b) may be written as

$$\sigma^2l^2+|\mu_1|V[\sigma V/(JV')-1]$$
$$\times\sigma l-\sigma V^3(\mu_1^2+\omega_1^2)/(JV')=0\ . \qquad (5.12c)$$

In dimensional units the criterion (5.12a) becomes

$$L_md=(\epsilon v_s/e\mu_0)l_m=8.85\times10^7l_m\ \mathrm{cm}^{-2}$$
$$\approx10^9\ \mathrm{cm}^{-2}\ (\text{for } p\text{-type Ge})\ . \qquad (5.12d)$$

For $d\approx10^{11}\ \mathrm{cm}^{-3}$, we find $L_m\approx0.1$ mm which is about 100 times smaller than the experimental samples of Kahn, Mar, and Westervelt.[7]

The minimal length formula (5.12) is more complicated than its counterpart in the classical model of the Gunn effect in n-type GaAs.[10,23] A source of ambiguities in its application to Ge is that we have considered the steady state to be uniform in space while $E(x)$ may be quite nonuniform as discussed in Sec. IV. We may take E_s to be some average of $E(x)$, but it is not clear which one we should use. For n-type GaAs it is possible to show that the minimal length that appears in the criterion (5.12) really means: the (weighted) length of the sample portion where $E(x)$ takes values on the NDR branch of $j(E)$ has to be larger than l_m for $E(x)$ to be linearly unstable.[24] For the model under study in this paper, we shall now *assume* that a similar criterion holds: Let l_{NDR} be the length of the interval where $E(x)$ takes values on the NDR branch of $j(E)$. Then $E(x)$ is linearly stable under voltage bias if $l_{\mathrm{NDR}}<l_m$ and linearly unstable otherwise.

An argument in support of this assumption is given in Appendix B. A proof should reveal whether a weighted average such as the flight time should be substituted for l_{NDR} in the previous statement. Taking this for granted, we shall now show that there exist two voltages ϕ_α and ϕ_ω, $E_1(J_c)l<\phi_\alpha<\phi_\omega<E_3(J_c)l$ (J_c is either J_M, J_{crit}, or J_m for cases A, B, or C in Sec. IV, respectively): For voltages outside the interval $(\phi_\alpha,\phi_\omega)$ the steady state is linearly stable, and it is linearly unstable for voltages inside this interval. This statement follows from the analysis of the steady state performed in Sec. IV. Take, for example, case B (the discussion of the other cases is analogous). Ignoring transition layers of width $O(1)$ as compared with $l\gg1$, $l_{\mathrm{NDR}}=\Delta x$ for $E_1(J_{\mathrm{crit}})l<\phi<E_2(J_{\mathrm{crit}})l$. ϕ_α is the voltage corresponding to $\Delta x=l_m$ in (4.9a). For larger ϕ, $E=E_2(J_{\mathrm{crit}})$ occupies a longer portion of the semiconductor, and the steady state is then linearly unstable. For $E_2(J_{\mathrm{crit}})l<\phi<E_3(J_{\mathrm{crit}})l$, $E=E_2(J_{\mathrm{crit}})$ if $0<x<\Delta x$, and Δx shrinks as ϕ increases: ϕ_ω is then the voltage corresponding to $\Delta x=l_m$ in (4.9b). For larger

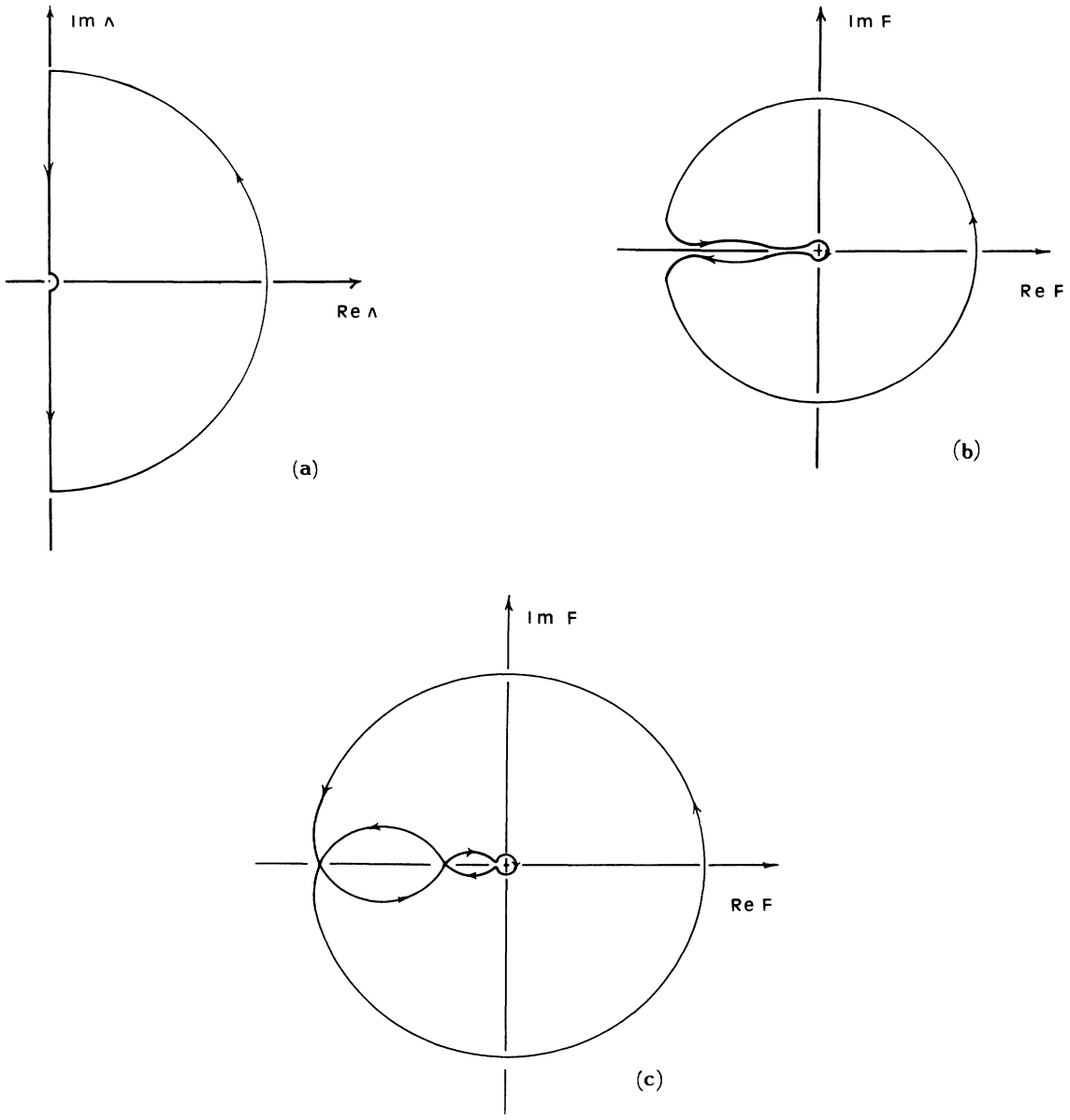

FIG. 5. (a) Curve enclosing the right half complex plane Λ but not the origin; (b) image of the curve depicted in (a) under the map $F(\Lambda)$ if $(b-c)<1-2/\pi$; and (c) same as in (b) if $(b-c)>1-2/\pi$ and $\mathrm{Im}F(i\omega)$ has two zeros for positive ω.

voltages, $\Delta x < l_m$, and the steady state is again linearly stable.

Let us end this section by noticing that only minimal modifications are needed to extend our analysis to more general boundary conditions. If the contact current density is a nonlinear function of the field, as in (4.12), the previous analysis and results hold with $\rho_0=[dJ_0(E_s)/dE]^{-1}$. If we adopt a constant field boundary condition, we just have to use $\rho_0=0$ in our results.

VI. DISCUSSION

In this paper we have derived a reduced equation for the electric field valid outside a narrow boundary layer at the receiving contact, for all values of the field (both above and below breakdown). We have found the unique steady state under dc voltage bias and qualitatively discussed how its shape changes according to the voltage and the boundary conditions. For a linear (Ohmic-) contact current density curve $J_0(E)$, the steady state lacks a voltage drop near the injecting contact [Fig. 3(a)] for certain values of the bias. This defect can be readily corrected without affecting our results by using a different $J_0(E)$ as explained in Secs. IV and V. We have also discussed the shape of the steady current-voltage characteristic diagram $J_{ss}(\phi)$. For all the boundary conditions considered, we have shown that this diagram is as in Fig. 4, with a (relatively) flat portion separating two regions where the

slope of $J_{ss}(\phi)$ is not small. A simplified linear stability analysis of the steady state has shown that it is linearly stable outside an interval of voltages belonging to the flat part of $J_{ss}(\phi)$. This latter feature is observed in the experiments [see Fig. 8 of Ref. 7: let us join the last points where there are no oscillations, corresponding to ϕ_α and ϕ_ω. The line thus obtained has a slope which is eight times smaller than that of the current-field diagram before the instability, and three times smaller than the slope of the current-field diagram after the instability. A similar calculation for $\alpha=1.4$ and $l=1000$ yields a relatively flat portion of the current-field diagram $J_{ss}(\phi)$ which has a slope ten times smaller than that of $J_{ss}(\phi)$ before it, and two times smaller than the slope of the current-field diagram after the flat portion. Since the numerical results are sensitive to the compensation ratio α, a quantity not reported in Ref. 7, we consider the agreement as satisfactory and do not try to improve it in the present paper]. A biproduct of our analysis is the minimal length criterion (5.12): for a semiconductor shorter than l_m the steady state is linearly stable. The samples in Refs. 6 and 7 are noticeably larger than the value 0.1 mm estimated for $d\approx 10^{11}$ cm^{-3}, and therefore the presence of instabilities is compatible with our criterion. Much shorter samples were used by Teitsworth[25] who reported that no instabilities could be observed on a sample with $L=0.5$ mm (see Table 3.2 and Fig. 3.1 of Ref. 25). When another sample of the same boule was cut with $L=4$ mm, spontaneous oscillations were observed.[25] This provides evidence in favor of our criterion (the estimate $L_m\approx 0.1$ mm is a rather gross one, given the lack of accurate curves for the transport coefficients and the approximations involved in our work).

Further understanding of the instabilities of the current in dc-biased extrinsic semiconductors should proceed along two lines. First a Hopf bifurcation analysis should reveal how oscillatory branches bifurcate from the steady state at the voltages ϕ_α and ϕ_ω. This analysis has been performed recently for n-type GaAs.[26] Were the present model to explain the experimental results,[7] the oscillatory branches bifurcating at ϕ_α and ϕ_ω (representing small amplitude oscillations of the current) should both be stable near the bifurcation points. The rest of our interpretation depends on the branch of solutions mediated by the motion of domains (solitary waves). So far we have been able to describe only the part of the oscillation period in which a domain moves far from the contacts,[20] not the stages of disappearance of a domain at the receiving contact and the formation of another one at $x=0$.[27] To understand the large amplitude oscillations of the current and the threshold behavior, one has to wait until the numerical and asymptotic analysis of the reduced equations derived in this paper are completed. With the present information it is possible however to qualitatively understand an interesting observation: why the frequency of the small amplitude oscillation of the current in the experiments[7] of Kahn, Mar, and Westervelt is higher than the frequency of the domain mediated oscillation.

Since the imaginary part of the zero of the impedance does not vanish at the critical voltages ϕ_α and ϕ_ω, it is plausible that Hopf bifurcations from the steady state occur at these values of the bias. The frequency of the oscillations at the threshold ϕ_α is

$$\begin{aligned}\Omega_{so}=\mathrm{Im}\lambda&=c_2\omega_1/[c_1 l+|\mu_1|]\\&\sim c_2\omega_1/(c_1 l)\\&=(K+R)V\omega_1/(V' l),\quad l\gg 1\ .\end{aligned}\tag{6.1}$$

Near threshold, small amplitude current oscillations are observed.[7] Assuming that they are described by a Hopf bifurcation from the steady state, their frequency should be close to (6.1). Besides small oscillations, current spikes caused by formation of domains are observed. The domain size varies as it moves towards $x=l$, and also the current varies. Nevertheless, let us estimate the frequency caused by domain dynamics by using the wave speed calculated for a domain moving with a constant current.[14] This speed was found to be larger than a value $C^*=(K+R)V/V'$, so that we estimate an angular frequency

$$\Omega_c\approx 2\pi C^*/l=2\pi(K+R)V/(V' l)\ .\tag{6.2}$$

It seems that the frequency of the spikes is of the same order as that of the small amplitude oscillation (6.1) when (5.8) is used. This however is illusory: (6.1) and (6.2) must be compared under the same dc voltage conditions ϕ. Then the current J_{so} corresponding to small oscillation about the steady state with voltage ϕ will be higher than the current J_d corresponding to a domain traveling over the steady state so that the total area under $E(x,\tau)$ is also ϕ. (J_d may be calculated from the current-voltage characteristic diagrams of both the steady state and the domain.[20]) Therefore the ratio between the frequencies (6.1) and (6.2) will be approximately,

$$\Omega_{so}/\Omega_d\approx(\omega_1/2\pi)[(K+R)V/V']_{J=J_{so}}/[(K+R)V/V']|_{J=J_d}\ .\tag{6.3}$$

Note that the frequency ratio is inversely proportional to the ratio of the mobilities at the electric fields $E_2(J)$ given by the corresponding values of the current J_{so} and J_d. Since the mobility decreases with the field and $E_2(J_{so})<E_2(J_d)$, the ratio (6.3) will be smaller than $\omega_1/2\pi$. Numerical evaluation for typical values of the parameters[28] yields a frequency ratio slightly larger than 1. Experimentally however, $\Omega_{so}/\Omega_d\approx 4$. What is the reason of this discrepancy?

We believe that the discrepancy is indirect evidence showing that the compensation ratio α is not a constant throughout the sample of Kahn, Mar, and Teitsworth,

but that, in fact, increases with x for most of the sample.[29] If this is so, as the solitary wave moves toward the receiving contact, its corresponding current must increase (the NDR region moves upward, to larger currents, as α increases, cf. Fig. 2). But then the velocity of the solitary wave diminishes (which accounts for the larger experimental value of Ω_{so}/Ω_d) and so does its size. This shrinking of the domains as they move is observed experimentally,[7] while preliminary numerical calculations[30] using the reduced equation (3.1) show that the sizes of the domains do not change after they reach maturity: typically a domain is formed a short time after $t=0$, moves toward the receiving contact, and starts leaving the sample when it reaches the receiving contact. Then the current goes up until another domain is created at $x=0$. The new domain moves toward $x=l$ and grows as it absorbs the area released by the old domain at $x=l$. As this process goes on, the current decreases slowly. After a certain amount of time and for long enough samples, the old domain has disappeared, the new one has reached maturity, and the current remains constant during the time it takes for the new domain to reach the receiving contact. See Fig. 6. We will present the results of our numerical simulations elsewhere.[30]

In conclusion, we have derived a reduced problem for the electric field that may describe the current instabilities in extrinsic semiconductors, both above and below the impurity breakdown field (except for a narrow diffusive boundary layer near the receiving contact). A rough linear stability analysis of the corresponding steady state shows that NDR is necessary for its linear instability both for $E>E_{br}$ and for $E<E_{br}$. As a consequence, instabilities below breakdown cannot appear as bifurcations from the steady state. The shape of the current-voltage characteristic $j(E)$ for uniform steady states then implies that the unique nonuniform steady state is unstable only between two critical voltages on the flat part of Fig. 4. We have derived also a minimal length criterion for the linear instability of the steady state and given a qualitative explanation of the larger frequency of the small amplitude current oscillations as compared to those due to motion of domains. The following open problems remain

Analysis of the current oscillations due to solitary-wave dynamics (domains). This analysis should be the equivalent of that for the classical model of the Gunn effect in n-type GaAs.[27]

Analysis of the bifurcation of oscillatory solutions at the lower and upper critical fields, and of the relation between the bifurcating branches and the solitary-wave branch.[20,26]

Precise comparison of these analyses with numerical simulations of the rate equations[30] based upon more accurate transport coefficients[28] and with the experiments.

We hope to tackle these problems in future publications

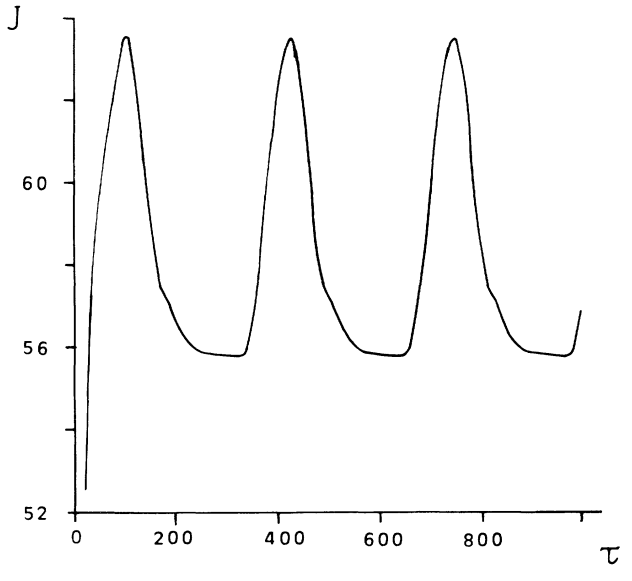

FIG. 6. Sample numerical calculation for $\alpha=1.15$; $\phi/l=0.79$ (corresponding to 7.9 V/cm); $\rho_0=13.43$. The vertical scale has been multiplied by 1000, so that to convert to dimensional units (in mA) we have to multiply each unit of J in the figure by 0.005 12. The absolute values of the current are extremely sensitive to the compensation ratio α. The frequency of this oscillation is about 0.23 kHz, which as it happens with the current, is too low compared with experiments. To obtain values of the current and the field compatible with the experimental ones, we must use α's between 1.4 and 1.51 (see Ref. 28).

ACKNOWLEDGMENTS

I thank Inma Rodriguez for providing the numerical results used in different parts of this paper. This work has been supported in part by the DGICYT under Grant No. PB89-0629, by the NATO traveling Grant No. CRG-900284, and by the Comité Conjunto Hispano-Norteamericano para la Cooperación Cultural y Educativa. I am indebted to the Gruppo Nazionale di Fisica Matematica of the Italian CNR for support during my stay at Padova and to Professor Renato Spigler for making it possible

APPENDIX A: NONDIMENSIONALIZATION OF GOVERNING EQUATIONS

We adopt the conventions of Ref. 14. The unknown and independent variables are defined by

$$\begin{aligned} &E=\mu_0\tilde{E}/v_s\ , \\ &P=p/d\ , \\ &A=a_*/d-1\ , \\ &J(\tau)=J_{\rm cot}(T)/(edv_s)\ , \\ &x=X/L_1=\mu_0 edX/(\epsilon v_s)\ , \\ &\tau=T/T_2=\kappa_0 dT\ . \end{aligned} \tag{A1}$$

Here L_1 is the typical length over which the electric field varies, as evaluated from Poisson's equation (1.1c). T_2 is the characteristic time for impact ionization of impurities, as estimated from the rate equation (1.1a). The

characteristic recombination time is also of the order of T_2. Insertion of (A1) into Eqs. (1.1a)–(1.1c), (1.2) and (1.3b) yields Eqs. (1.4a)–(1.4c), (1.5) and (1.6), where

$$\phi=-\mu_0^2 ed\tilde{V}/(\epsilon v_s^2)\ ,$$

$$\rho_n=(e\mu_0 d)\times(\text{resistivity of contact } X=nL)\ ,$$

$$n=0,1\ ,$$

$$\alpha=a/d>1 \text{ (compensation ratio)}\ ,$$

$$\delta=\mu_0 e\, dD/(\epsilon v_s^2)=\mu_0^2 dk_B T_0/(\epsilon v_s^2)\approx 10^{-2}\ , \qquad \text{(A2)}$$

$$l=\mu_0 e\, dL/(\epsilon v_s)\approx 10^3\ ,$$

$$\Gamma/\beta=\gamma T_2=\gamma/(\kappa_0 d)\approx 10^{-1}-10^{-5}\ ,$$

$$\beta=T_1/T_2=\epsilon\kappa_0/(e\mu_0)\approx 2.5\times 10^{-5}\ .$$

Here we have indicated typical numerical values appropriate to p-type Ge. β is the ratio between the dielectric relaxation time $T_1=\epsilon/(e\, d\mu_0)$ and the impurity time $T_2=1/(\kappa_0 d)$.

APPENDIX B: LINEAR STABILITY OF NONUNIFORM STEADY STATES ON LONG SAMPLES

A linear stability analysis of the nonuniform steady state on long enough samples may be performed by adapting Kroemer's for the classical model of the Gunn effect in n-type GaAs.[19] We shall consider case B of Sec. IV B, so that E/ρ_0 and $j(E)$ intersect on the two first branches of the latter. For $l\gg 1$ and α not too close to 1 (say, $\alpha=1.4$), the steady state consists of two plateaus joined by a transition region of width $O(1)E$ is $E_2(J_{\rm crit})$ for $0<x<\Delta x$, and E is either $E_1(J_{\rm crit})$ or $E_3(J_{\rm crit})$ for $\Delta x<x<l$, according to whether

$$E_1(J_{\rm crit})l<\phi<E_2(J_{\rm crit})l\ ,\quad J\uparrow J_{\rm crit}$$

$$\text{or } E_2(J_{\rm crit})l<\phi<E_3(J_{\rm crit})l\ ,\quad J\downarrow J_{\rm crit}$$

Δx is given by (4.9a) or (4.9b), respectively. We now show that the steady state becomes linearly unstable for voltages such that the width of the interval for which $E(x)$ is in the NDR region of $j(E)$ is small compared to l. Let us start with a small voltage for which Δx is given by (4.9a) and ignore the $O(1)$ transition region as compared to the width of the two plateaus. The solution of the linear equation (5.2a) is

$$\hat{e}(x)=\rho_0\exp(-\Lambda_2 x/\Delta x)+[1-\exp(-\Lambda_2 x/\Delta x)]\times\Delta x/(\Lambda_2 V_2)\ ,\quad 0<x<\Delta x\ , \qquad \text{(B1a)}$$

$$\hat{e}(x)=\hat{e}(\Delta x)\exp[-\Lambda_1(x-\Delta x)/l]+\{1-\exp[-\Lambda_1(x-\Delta x)/l]\}l/(\Lambda_1 V_1)\ ,\quad \Delta x<x<l\ , \qquad \text{(B1b)}$$

$$\Lambda_1=(\lambda c_1+c_4)l/(\lambda+c_2)\ , \qquad \text{(B1c)}$$

$$\Lambda_2=(\lambda c_1+c_4)\Delta x/(\lambda+c_2)\ . \qquad \text{(B1d)}$$

The subscripts 1 and 2 in V and Λ mean that the functions of E that appear are to be evaluated at $E_1(J_{\rm crit})$ and $E_2(J_{\rm crit})$, respectively. Insertion of (B1) in the bias condition yields $Z(\lambda)=0$, where

$$V_1\Lambda_1 Z(\lambda)/l^2=(\Lambda_1/l-\{1-\exp[-\Lambda_1(1-\Delta x/l)]\}\Lambda_2/\Delta x)V_1 Z_1(\Lambda_2)/l+1-\Delta x/l+\{1-\exp[-\Lambda_1(1-\Delta x/l)]\}\{[\rho_0+\Delta x/V_2]V_1/l-1/\Lambda_1\}\ , \qquad \text{(B2a)}$$

$$Z_1(\Lambda)/l=(\Delta x)^2[\Lambda+e^{-\Lambda}-1-\rho_0 V_2\Lambda(e^{-\Lambda}-1)/\Delta x]/(V_2 l\Lambda^2)\ . \qquad \text{(B2b)}$$

From (B1d) we find (5.6) with $\Lambda=\Lambda_2$ and Δx instead of l. Clearly, if $\Lambda_2\gg\Delta x$ ($\Lambda_2\ll\Delta x$), then $\lambda\sim -c_2(E_2)<0$ [$\lambda\sim-(c_4/c_1)|_2>0$] and the steady state is linearly stable (unstable). (B2) may now be used to prove that $\Lambda_2\gg\Delta x$ ($\Lambda_2\ll\Delta x$) follows from $\Delta x\ll\ln l$ ($\Delta x\gg\ln l$). A more precise analysis shows that the steady state is linearly unstable if and only if $\Delta x>l_m$ where

$$l_m\sim(V_2/\sigma_2)\ln l,\quad \sigma_2=|dj(E_2)/dE|\ . \qquad \text{(B3)}$$

Substitution of this value of Δx in (4.9a) yields ϕ_α:

$$\phi_\alpha\sim E_1 l+(E_2-E_1)(V_2/\sigma_2)\ln l\quad (J=J_{\rm crit})\ . \qquad \text{(B4a)}$$

The zero of the impedance $Z(\lambda)$ with smallest $|{\rm Re}\Lambda_2|$ is reached at

$$\Lambda_1\sim\sigma_1 l/V_1,\quad \sigma_1=dj(E_1)/dE>0\ , \qquad \text{(B5a)}$$

$$\Lambda_2\sim\pm i\pi+\ln\{(1+\rho_0\sigma_2)(V_1\sigma_2+V_2\sigma_1)/(\sigma_2^2 l)\}\ . \qquad \text{(B5b)}$$

The same analysis for larger voltages such that the second plateau is $E=E_3(J_{\rm crit})$ yields the critical voltage ϕ_ω above which the steady state is again linearly stable. We determine it from (4.9b) with $\Delta x=l_m$ given by (B3):

$$\phi_\omega\sim E_3 l-(E_3-E_2)(V_2/\sigma_2)\ln l\quad (J=J_{\rm crit})\ . \qquad \text{(B4b)}$$

*Present address.
[1]E. Scholl, Phys. Rev. B **32**, 1395 (1985).
[2]K. Aoki and K. Yamamoto, Phys. Lett. **98A**, 72 (1973).
[3]J. Peinke, A. Muhlbach, R. P. Huebener, and J. Parisi, Phys. Lett. **108A**, 407 (1985).
[4]D. G. Seiler, C. L. Littler, R. J. Justice, and P. W. Milonni, Phys. Lett. **108A**, 462 (1985).
[5]E. G. Gwinn and R. M. Westervelt, Phys. Rev. Lett. **57**, 1060 (1986).
[6]A. M. Kahn, D. J. Mar, and R. M. Westervelt, Solid State Electron. **32**, 1143 (1989).
[7]A. M. Kahn, D. J. Mar, and R. M. Westervelt, Phys. Rev. B **43**, 9740 (1991).
[8]K. M. Mayer, R. Gross, J. Parisi, J. Peinke, and R. P. Huebener, Solid State Commun. **63**, 55 (1987); K. M. Mayer, J. Parisi, and R. P. Huebener, Z. Phys. B **71**, 171 (1988).
[9]J. B. Gunn, in *Proceedings of the Symposium on Plasma Effects in Solids, Paris, 1964* (Dunod, Paris, 1965), p. 199.
[10]M. P. Shaw, H. L. Grubin, and P. R. Solomon, *The Gunn-Hilsum Effect* (Academic, New York, 1979).
[11]L. L. Bonilla, SIAM J. Appl. Phys. Math. **51**, 727 (1991); L. L. Bonilla and F. J. Higuera, Physica D **52**, 458 (1991).
[12]S. W. Teitsworth, Appl. Phys. A **48**, 127 (1989).
[13]B. K. Ridley, Proc. Phys. Soc. **82**, 954 (1963).
[14]L. L. Bonilla and S. W. Teitsworth, Physica D **50**, 545 (1991).
[15]B. W. Knight and G. A Peterson, Phys. Rev. **147**, 617 (1966).
[16]A. F. Volkov and Sh. M. Kogan, Usp. Fiz. Nauk **96**, 633 (1968) [Sov. Phys. Usp. **11**, 881 (1969)].
[17]L. L. Bonilla and J. M. Vega, Phys. Lett. A **156**, 179 (1991).
[18]H. L. Grubin, IEEE Trans. Electron. Dev. **ED-23**, 1012 (1976).
[19]H. Kroemer, IEEE Trans. Electron. Dev. **ED-15**, 819 (1968).
[20]L. L. Bonilla, Physica D **55**, 182 (1992).
[21]L. M. Lambert, J. Phys. Chem. Solids **23**, 1481 (1962).
[22]R. Bellman and K. L. Cooke, *Differential-Difference Equations* (Academic, New York, 1963), Chaps. 12 and 13.
[23]D. E. McCumber and A. G. Chynoweth, IEEE Trans. Electron. Dev. **ED-13**, 4 (1966).
[24]M. P. Shaw, H. L. Grubin, and P. R. Soloman, *The Gunn-Hilsum Effect* (Ref. 10), Chap. 6. For GaAs, $j(E)=v(E)$. For a piecewise linear $v(E)$, l_m is the flight time $\int dx/v(E(x))$, where the integral is evaluated over x such that $dv(E(x))/dE<0$.
[25]S. W. Teitsworth, Ph.D. thesis, Harvard University, 1986.
[26]The analysis of the Hopf bifurcation for the simpler model of n-type GaAs has been performed in L. L. Bonilla (unpublished). The list of all the bifurcation diagrams which are possible for the instability (Fig. 3) is equally applicable to p-type Ge, as we will explain elsewhere.
[27]This is known for the classical model of n-type GaAs, but not yet for p-type Ge. See F. J. Higuera and L. L. Bonilla, Physica D (to be published).
[28]X. Zhang, S. W. Teitsworth, and L. L. Bonilla (unpublished).
[29]Private discussions with A. M. Kahn, D. Mar, and S. W. Teitsworth.
[30]L. L. Bonilla, I. Rodriguez, and S. W. Teitsworth (unpublished).